HHS Public Access

Author manuscript

Cancer Prev Res (Phila). Author manuscript; available in PMC 2023 July 04.

Published in final edited form as:

Cancer Prev Res (Phila). 2023 January 04; 16(1): 17–28. doi:10.1158/1940-6207.CAPR-22-0332.

Treatment strategies and mechanisms associated with the prevention of NASH-associated HCC by a toll-like receptor 4 inhibitor

Suet-Ying Kwan[1], **Alyssa N. Slayden**[1], **Aubrey R. Coronado**[1], **Rosamaria C. Marquez**[1], **Huiqin Chen**[2], **Peng Wei**[2], **Michelle I. Savage**[3], **Lana A. Vornik**[3], **Jennifer T. Fox**[4], **Shizuko Sei**[4], **Dong Liang**[5], **Heather L. Stevenson**[6], **Gregory K. Wilkerson**[7], **Mihai Gagea**[8], **Powel H. Brown**[3], **Laura Beretta**[1]

[1]Department of Molecular and Cellular Oncology, The University of Texas MD Anderson Cancer Center, Houston, Texas, USA

[2]Department of Biostatistics, The University of Texas MD Anderson Cancer Center, Houston, Texas, USA

[3]Department of Clinical Cancer Prevention, The University of Texas MD Anderson Cancer Center, Houston, Texas, USA

[4]Chemopreventive Agent Development Research Group, Division of Cancer Prevention, National Cancer Institute, Rockville, Maryland, USA

[5]Department of Pharmaceutical Sciences, College of Pharmacy and Health Sciences, Texas Southern University, Houston, Texas, USA

[6]Department of Pathology, The University of Texas Medical Branch, Galveston, Texas, USA

[7]Keeling Center for Comparative Medicine and Research, University of Texas, MD Anderson Cancer Center, Bastrop, Texas, USA

[8]Department of Veterinary Medicine & Surgery, The University of Texas MD Anderson Cancer Center, Houston, Texas, USA

Abstract

We evaluated the cancer preventive efficacy of TAK-242, an inhibitor of toll-like receptor 4 (TLR4), in a mouse model of hepatocellular carcinoma (HCC) occurring in the context of non-alcoholic steatohepatitis (NASH). We also assessed the cellular events associated with the preventive treatment efficacy. We tested oral administration of TAK-242, at clinically-relevant

Correspondence: Laura Beretta, Ph.D., Department of Molecular and Cellular Oncology, The University of Texas MD Anderson Cancer Center, 1515 Holcombe Boulevard, Houston, TX 77030, USA. Tel.: +1 713 792 9100: lberetta@mdanderson.org.

AUTHOR CONTRIBUTIONS

Conceptualization: J.T.F., S.S., P.H.B., L.B.; Methodology: S.K., A.R.C., H.C., P.W., D.L.; Formal Analysis: S.K., A.N.S., H.C., P.W., D.L., H.L.S., G.K.W., M.G., L.B.; Investigation: S.K., A.N.S., A.R.C., R.C.M., D.L., H.L.S., G.K.W., M.G.,; Resources: D.L.; Writing – original draft: S.K., A.N.S., L.B.; Writing – review and editing: S.K., A.N.S., A.R.C., R.C.M., H.C., P.W., M.I.S., J.T.F., S.S., D.L., H.L.S., G.K.W., M.G., P.H.B., L.B.; Visualization: S.K., A.N.S., L.B.; Supervision: M.I.S., L.A.V., J.T.F., S.S., P.H.B., L.B.; Funding Acquisition: P.H.B., L.B..

Conflict of interest:

The authors declare no potential conflicts of interest.

but toxicity-reducing doses and scheduling, in mice with hepatocyte-specific deletion of *Pten* (Hep*Pten*$^{-}$). The optimal dose and oral gavage formulation of TAK-242 were determined to be 30 mg/kg in 5% DMSO in 30% 2-hydroxypropyl-β-cyclodextrin. Daily oral administration of 30 mg/kg TAK-242 over 18 weeks was well-tolerated and resulted in reduced development of tumors (lesions >7.5 mm^3) in Hep*Pten*$^{-}$ mice. This effect was accompanied by reduced macrovesicular steatosis and serum levels of alanine aminotransferase (ALT). In addition, 30 mg/kg TAK-242 daily treatment of small pre-existing adenomas (lesions <7.5 mm^3) over 18 weeks, significantly reduced their progression to HCC. RNA sequencing identified 220 hepatic genes significantly altered upon TAK-242 treatment, that significantly correlated with tumor burden. Finally, cell deconvolution analysis revealed that TAK-242 treatment resulted in reduced hepatic populations of endothelial cells and myeloid-derived immune cells (Kupffer cells, Siglec-H high dendritic cells and *NGP* high neutrophils), while the proportion of *MT-ND4* high hepatocytes significantly increased, suggesting a decrease in hepatic inflammation and concomitant increase in mitochondrial function and oxidative phosphorylation upon TLR4 inhibition. In conclusion, this study identified treatment strategies and novel molecular and cellular mechanisms associated with the prevention of HCC in the context of NASH that merit further investigations.

Keywords

TLR4; TAK-242; non-alcoholic steatohepatitis; hepatocellular carcinoma; cancer prevention

INTRODUCTION

HCC is a fast-growing cause of cancer-related deaths in the United States (U.S) (1). While viral hepatitis and alcohol consumption remain common etiologies of HCC, non-alcoholic fatty liver disease (NAFLD) is becoming a prevalent risk factor for HCC (2, 3). NAFLD is the liver manifestation of obesity and diabetes and the most common chronic liver disease in the U.S. (4). Starting with simple steatosis, NAFLD can advance to NASH, advanced liver fibrosis/cirrhosis and HCC. NASH patients with advanced liver fibrosis/cirrhosis are at high risk for HCC. The fast-growing incidence of HCC is largely due to the epidemics of obesity and diabetes (2, 5). Most HCCs are diagnosed at a late stage and the overall prognosis is poor, with a 5-year survival rate of 20% (6). Prevention is therefore an important priority to reduce HCC mortality and reverse the current trend of increasing incidence rates in the U.S. To date, there are no approved treatments for NASH or liver fibrosis. While potential strategies for HCC chemoprevention have been evaluated (aspirin, anti-diabetic drugs, statins, pre- and probiotics) (7, 8), few studies have examined the effect of HCC prevention specifically in the context of NASH.

Hep*Pten*$^{-}$ mice develop NASH, liver fibrosis and HCC (9, 10). We identified TLR4 as the primary driver of HCC development in Hep*Pten*$^{-}$ mice, and TAK-242, a small molecule TLR4 inhibitor, as the primary candidate drug for the prevention of NASH-associated HCC (11). We further showed that HCC development was reduced in Hep*Pten*$^{-}$ mice receiving daily intraperitoneal (IP) injections of TAK-242 for 28 days (11). TLR4 is a proinflammatory receptor for gut bacteria-derived lipopolysaccharide (LPS) and

other pathogen-associated molecular patterns. In the liver, TLR4 is expressed by both hepatocytes and non-parenchymal cells. Dysregulation of TLR4 signaling leads to abnormal inflammatory responses, with implications for NASH progression and liver fibrosis. Increased circulating and hepatic LPS levels have been observed in NASH patients (12). *In vivo* studies demonstrated that LPS/TLR4 signaling promotes liver fibrosis and hepatocarcinogenesis, enhanced expression of the proinflammatory cytokines interleukin-6 (IL-6) and tumor necrosis factor-α (TNF-α), and increased fibronectin production in hepatic stellate cells, leading to extracellular matrix and vascular changes (13, 14). Activation of TLR4/NF-κB signaling in liver has also been shown to promote the accumulation of reactive oxygen species, hepatic inflammatory responses and liver fibrosis (15–17). Finally, TLR4 signaling has been associated with hepatocarcinogenesis in chemically-induced mouse models of HCC (18–20).

TAK-242 binds to Cys^{747} in the intracellular domain of TLR4 to inhibit intracellular signaling (21). While initially developed for the treatment of sepsis, TAK-242 has been reported to confer hepatic protection. TAK-242 decreased LPS-induced cytokine secretion by hepatic stellate cells, monocytes and hepatocytes *in vitro* (22, 23) and reduced circulating cytokine levels *in vivo* (23). TAK-242 may also confer hepatoprotection through its effects on oxidative stress (24, 25). I*n vitro* studies suggested an anti-tumor effect of TAK-242, due to suppressed expression of hypoxia-inducible factor-1α and reduced invasive potential of HCC cell lines (26, 27).

Herein, we determined the optimal formulation for oral delivery of TAK-242, as well as its tolerability and efficacy in preventing HCC in the Hep*Pten*$^{-}$ model of NASH-associated HCC. We also determined the efficacy of TAK-242 in preventing progression of small adenomas to HCC. Finally, we identified the molecular and cellular mechanisms associated with TAK-242-induced HCC prevention.

MATERIALS AND METHODS

TAK 242 Formulation and Measurement

TAK-242 was sourced from Accel Pharmtech (WW1401, lot 2716), with purity of 99.31% by liquid chromatography (LC)-mass spectrometry (MS) and 99.40% by enantiomeric excess. Formulations tested for oral gavage were: 0.5% methylcellulose, 5% dimethyl sulfoxide (DMSO) in 30% 2-hydroxypropyl-β-cyclodextrin (2-HPβCD), 20% Captisol, 1% carboxymethyl cellulose (CMC) and 0.5% Tween-80 in water, and 0.5% hydroxypropylmethylcellulose (HPMC) and 0.2% Tween-80 in water. The formulation for IP injection was 1% DMSO in phosphate-buffered saline. Blood was collected by retro-orbital bleeding 2 hrs after drug administration. For TAK-242 measurements, pooled plasma samples (20 μL) were mixed with an internal standard (bromfenac, 15μL of 40 ng/mL in 50% acetonitrile). Protein was precipitated by adding 400 μL of ethyl acetate, vortexed, and centrifuged at 13,000 rpm, 4°C for 15 min. Supernatant was transferred into a glass tube, dried under N_2 gas, reconstituted with 100 μL 50% acetonitrile, vortexed and centrifuged, before injection (2 μL) onto a LC-MS/MS system. Chromatography separation was accomplished on a Shimadzu Nexera X2 UHPLC system (Columbia, MD) equipped with ACE Excel 2 Super C_{18} column (50×2.1 mm ID, 2.7 μm) using a gradient mobile phase

at 0.5 mL/min flow rate, with component A (0.1% v/v formic acid in water) and component B (0.1% v/v formic acid in acetonitrile). Gradient elution was: 20% B for 0–0.2 min, 20% to 98% B for 0.2–2.5 min, 98% B for 2.5–3.5 min, 20% B for 3.5–3.6 min, and 20% B for 3.6–4.6 min. MS/MS analysis was performed on a 4000 QTRAP® triple quadrupole MS system equipped with a Turbo Ion Spray ion source (SCIEX, Redwood City, CA) and operated in negative ion electrospray mode. Retention times for TAK-242 and bromfenac were 2.31 min and 2.14 min, respectively. The method was validated with a linear analytical range of 0.32–20.0 ng/mL TAK-242 in mouse plasma. TAK-242 concentrations in 5% DMSO in 30% 2-HPβCD were measured on an ACQUITY UPLC H-Class Plus system (Waters Corporation, Palatine, IL) using a Xterra MS C_{18} (4.6×150 mm, 3.5 μm) column with 60% acetonitrile in water containing 0.1% formic acid at 1 mL/min and monitored at 280 nm. The assay was linear in TAK-242 concentrations of 1.0–50.0 μg/mL.

Mice Treatment and MR Imaging

All animal procedures were carried out in accordance with the policies and regulations of the Institutional Animal Care and Use Committee (IACUC) at the University of Texas MD Anderson Cancer Center. Control and experimental mice were *Pten*$^{loxP/+}$;Albumin (Alb)-Cre^{+} and *Pten*$^{loxP/loxP}$;Alb-Cre^{+} (Hep*Pten*$^{-}$), respectively, and were obtained through the crossing of *Pten*$^{loxP/loxP}$;Alb-Cre^{+}male mice and *Pten*$^{loxP/+}$;Alb-Cre^{+} female mice (C57BL/6 background). Pharmacokinetic (PK) and tolerability studies were performed using 36 Hep*Pten*$^{-}$ and 36 control male mice, 8 months of age (n=3 per treatment group). In multi-dose studies, we tested daily oral administration of 3, 10 and 30 mg/kg of TAK-242 over 5 days, solubilized in 5% DMSO in 30% 2-HPβCD for oral administration. Mice in single-dose treatment groups were sacrificed after 12 or 24 hrs. For multi-dose treatment groups, mice were sacrificed 2 hrs after last dose. Efficacy studies were performed using 80 Hep*Pten*$^{-}$ male mice (n=10 per treatment group). Enrollment criteria were 8-month old male mice showing no lesion by MRI (Arm 1) or showing small liver lesions (<7.5 mm3 volume) by MRI (Arm 2). Hep*Pten*$^{-}$ mice were treated with TAK-242 solubilized in 5% DMSO in 30% 2-HPβCD by daily (Monday–Friday) oral gavage (10 ml/kg) at 3, 10 and 30 mg/kg, or placebo for 18 weeks. Mice were monitored for body weight and by MRI (Bruker Biospec USR47/40) every 14 days. Liver tumors were detected using a standard acquisition protocol with a 250 μm slice thickness and enough slices to cover the entire liver. The number of tumors and tumor volumes assessed by MRI were used to generate tumor incidences, calculated as the number of mice without tumors ≥7.5 mm^3 divided by the number of mice in the group.

Necropsies, Histology Analyses and Liver Function Assays

Blood was collected at necropsy by cardiac puncture. Spleen, kidney and liver tissues were harvested, weighed and fixed in 10% neutral formalin. Liver tumors were collected, and tumor diameters were measured. Tumor and liver sections were also snap-frozen in liquid nitrogen. Formalin-fixed tissue sections were sectioned and stained with hematoxylin and eosin and/or Masson's Trichrome. Histopathologic analysis was performed blindly by pathologists. We adopted the NAFLD Activity Score (NAS) (28) to include both macrovesicular and microvesicular steatosis grades, calculated as an unweighted sum of macrosteatosis (0–3), microsteatosis (0–3), lobular inflammation (0–3) and ballooning (0–2)

scores. Bile ductular reaction and liver fibrosis were also assessed on a 0–3 and 0–4 scale, respectively. Aspartate aminotransferase (AST) and ALT measurements in serum (30 μL of 6-fold dilution) were determined using the ACE Axcel clinical chemistry system (Diagnostic Technologies).

RNA Sequencing and Cell Deconvolution

RNA sequencing was performed on liver tissue from mice treated with placebo or 30 mg/kg TAK-242 for 18 weeks. Total RNA was extracted from snap-frozen livers using the miRNeasy Mini Kit (Qiagen). Following cDNA synthesis, end repair, adaptor ligation and PCR amplification with the KAPA Stranded mRNA-Seq kit, the enriched cDNA libraries were subjected to strand-specific mRNA sequencing on the Illumina NovaSeq 6000 system, using the SP flow cell and 100 base-pair paired-end reads. Sequence files were generated in FASTQ format (bcl2fastq, v2.20.0). Using the STAR (RRID:SCR_004463) program (v2.7.0f), raw reads were aligned to the mouse reference genome GRCm39 and the number of aligned read per gene using the annotations GRCm39.103 were counted. Genes with maximum abundance below 0.5 counts per million (CPM) across all samples were excluded, leaving 16,940 genes for differential expression analysis.

Statistical Analyses

Statistical differences in continuous variables between treatment groups were assessed by two-tailed, unpaired *t*-tests for normally distributed variables, or the Mann-Whitney *U* test for variables not normally distributed. Statistical differences in tumor incidences between treatment groups were assessed by Fisher's exact test. Differences in tumor-free survival between groups were assessed by the log-rank test. The Mann-Whitney *U* test was performed to identify genes differentially expressed genes (DEGs) in liver of mice treated with placebo or 30 mg/kg TAK-242 for 18 weeks. The criteria for DEGs were Mann-Whitney $p<0.05$ and FC ≥ 1.5 or ≤ -1.5. Spearman's correlation was performed between expression of each gene and tumor burden, with genes considered significantly correlated with tumor burden if they had a Spearman's correlation $p<0.05$. To impute relative proportions of cell populations in each liver sample, CIBERSORTx (29) was implemented using RNA sequencing data normalized to CPM. The reference signature matrix for adult mouse liver was obtained at: https://github.com/Nanostring-Biostats/CellProfileLibrary (30). For all tests, $p<0.05$ was considered significant.

Data Availability

The data generated in this study are available upon request from the corresponding author.

RESULTS

Optimal Oral Formulation, PK Studies and Drug Tolerability

As oral administration is the optimal route of drug delivery for chemoprevention, we first tested different formulations for oral administration of TAK-242, in control mice with three mice per formulation and a dose of 15 mg/kg. The formulations tested were: 0.5% methylcellulose, 5% DMSO in 30% 2-HPβCD, 20% captisol, 1% CMC and 0.5% Tween-80, and 0.5% HPMC and 0.2% Tween-80. An additional group of three mice

received 15 mg/kg TAK-242 in 1% DMSO by IP injection. Blood was collected by retro-orbital bleeding 2 hrs after drug administration, and TAK-242 was quantified by LC-MS/MS. Mice treated with TAK-242 in 5% DMSO in 30% 2-HPβCD had the highest plasma concentrations of TAK-242, with levels comparable to mice treated via IP injection (Fig. 1A). The solubility of TAK-242 in this formulation was assessed by high-performance liquid chromatography (HPLC) (Fig. 1B). Concentrations tested ranged from 15.625 to 3000 μg/mL (equivalent to a mouse dosage of 0.156–30 mg/kg) and the actual concentrations of dissolved TAK-242 were compared to the expected concentrations. TAK-242 demonstrated good solubility in the selected oral formulation as the actual concentration continued to increase up to 3000 μg/ml, where 33.4% of expected TAK-242 was detected. Therefore, 5% DMSO in 30% 2-HPβCD was selected as the vehicle for oral gavage in all subsequent experiments.

PK studies included both single and multi-dose treatments over 5 days and were performed on both 8-month old control and Hep*Pten*$^{-}$ male mice (n=72). Three control and three Hep*Pten*$^{-}$ mice were used per treatment group and collected plasma was pooled. As 30 mg/kg is the maximum tolerable dose, we tested oral administration of 3, 10 and 30 mg/kg TAK-242. In single-dose studies, blood was collected by retro-orbital procedure at 4, 12 and 24 hrs post-treatment. In multi-dose studies with daily oral administration of TAK-242 over 5 days, blood was collected 2 hrs after final administration. TAK-242 concentrations at 4 hrs were higher in Hep*Pten*$^{-}$ mice compared to control mice for the 10 and 30 mg/kg treatment groups (Fig. 1C). The single-dose 30 mg/kg TAK-242 in Hep*Pten*$^{-}$ mice had the highest concentration at 3.71 ng/mL compared to 3.41 ng/mL in control mice. Hep*Pten*$^{-}$ mice receiving multiple doses of 10 or 30 mg/kg TAK-242 also had higher plasma concentrations of the drug (2.05 and 1.66 ng/mL) compared to control mice (0.24 and 0.67 ng/mL) (Fig. 1D). As Hep*Pten*$^{-}$ mice present with NASH by 8 months of age, the higher plasma concentrations of TAK-242 in these mice compared to control mice, several hours after treatment, may reflect reduced hepatic drug clearance capacity.

Drug tolerability was assessed by organ weight, tissue histology, and hematologic and serum chemistry measurements. Liver, spleen and kidney weights at necropsy were normalized to body weight (Supplementary Fig. S1). No consistent changes in normalized organ weights were observed for any treatment group when compared to placebo. A slight but significant increase in kidney weight was observed in Hep*Pten*$^{-}$ mice treated by 3 mg/kg TAK-242 for 24 hrs ($p=0.027$). However, such increase was not observed in control mice nor in Hep*Pten*$^{-}$ mice treated with 10 or 30 mg/kg TAK-242 for 24 hrs. Most importantly, no changes in organ weights were observed in mice within the multi-dose treatment groups. No significant histological abnormalities in spleen or kidney were observed in any treatment group (Supplementary Table S1). The 30 mg/kg TAK-242 treatment group showed mild increased extramedullary hematopoiesis in spleen. Overall, the optimal dose and oral formulation of TAK-242 was determined to be 30 mg/kg in 5% DMSO in 30% 2-HPβCD, which was well-tolerated over 5 days of daily treatment.

Determination of TAK-242 Efficacy in Preventing HCC Development in Hep*Pten*$^{-}$ Mice

To determine the efficacy of TAK-242 in preventing HCC development, 8 month-old Hep*Pten*$^{-}$ male mice with no liver lesions detected by MRI, were enrolled and divided into 4 treatment groups (n=10 per group): placebo, 3, 10 and 30 mg/kg TAK-242. Treatment was orally administered daily for 18 weeks. There was no reduction in body weight in any treatment group throughout the study (Supplementary Fig. S2). Similarly, no difference was observed in liver or spleen weights at end of treatment, demonstrating no toxicity over 18 weeks for any of the doses tested. All mice were monitored by MRI every 2 weeks until end of treatment. For tumor endpoint analysis, liver lesions with volume <7.5 mm^3 were excluded. TAK-242 treatment resulted in a dose-dependent delay in tumor development. Liver tumors were first detected after 2 weeks of treatment only in 1 of the 10 mice from the placebo group. Liver tumors were detected after 6 weeks in 1 of the 10 mice treated with 3 mg/kg TAK-242 and in 3 of the 10 mice treated with 10 mg/kg TAK-242. Among the 10 mice treated with 30 mg/kg TAK-242, liver tumors were first detected after 8 weeks in only 2 mice. At end of treatment, 90%–100% of the mice in placebo, 3 and 10 mg/kg TAK-242 treatment groups had tumors, while only 77% of the mice in the 30 mg/kg TAK-242 treatment group had tumors (Fig. 2A). The delay in tumor development in mice treated with 30 mg/kg TAK-242 was further demonstrated by tumor-free survival curves. Although not significantly, mice treated with 30 mg/kg TAK-242 had a median tumor-free survival time of 98 days compared to 70 for mice in the placebo group (Fig. 2B). The average number of tumors per mouse at end of treatment was also lower in mice treated with 30 mg/kg TAK-242 (2.22±0.62 compared to 4.11±1.06 in the placebo group) (Fig. 2C). Tumor burden, measured by MRI at 18 weeks, was also reduced in mice from all TAK-242 treatment groups compared to placebo, with statistical significance and strongest reduction (5.1-fold) observed for mice treated with 30 mg/kg TAK-242 (Fig. 2D). The average tumor burden was 448.7±154.2, 148±50.1, 245.2±126.2 and 87.7±50.4 mm^3 for mice in the placebo, 3, 10, and 30 mg/kg of TAK-242 treatment groups, respectively (p=0.043). Individual tumor volumes were also strongly reduced in all TAK-242 treatment groups compared to placebo with the strongest reduction (2.7-fold) observed in the 30 mg/kg group (Fig. 2D). The average tumor volume was 79.0±15.9, 38.7±8.6 (p=0.012), 56.4±9.1, and 29.4±7.4 (p=0.001) mm^3 for placebo, 3, 10 and 30 mg/kg TAK-242 treatment groups, respectively (p=0.001). Necropsy results confirmed the end of treatment MRI results. Tumor burden was strongly reduced in all TAK-242 treated groups compared to placebo, with the strongest reduction (6.6-fold) observed in the 30 mg/kg TAK-242 treatment group (Fig. 2E). The average tumor burden was 624.6±237.5, 143.5±48.0, 257.2±121.6, and 94.6±56.2 (p=0.022) mm^3 for placebo, 3, 10 and 30 mg/kg TAK-242 treatment groups, respectively. Individual tumor volumes were strongly and significantly reduced in all TAK-242 treatment groups compared to placebo, with the strongest reduction observed in the 30 mg/kg group and corresponding to a 3.9-fold reduction (Fig. 2E). The average tumor volume was 160.1±59.3, 41.7±14.1 (p<0.001), 65.9±19.8 (p=0.023) and 37.9±14.9 (p=0.009) mm^3 for placebo, 3, 10 and 30 mg/kg TAK-242 treatment groups, respectively. These data indicated that 18-week treatment of Hep*Pten*$^{-}$ mice with TAK-242 was well-tolerated and resulted in reduced development of tumors, with the strongest effects observed with 30 mg/kg.

TAK-242 Treatment Efficacy in Preventing HCC Development from Small lesions in Hep*Pten*$^{-}$ mice

Additionally, we tested the efficacy of TAK-242 in preventing HCC progression from small lesions (adenomas) in Hep*Pten*$^{-}$ mice (Fig. 3). Eight-month-old Hep*Pten*$^{-}$ male mice with small adenomas <7.5 mm^3 detected by MRI, were enrolled and divided into 4 treatment groups (n=10 per group): placebo, 3, 10, and 30 mg/kg TAK-242. There was no statistical difference in tumor burden among the treatment groups at start of treatment (Fig. 3A). All small lesions at start of treatment were monitored by MRI every 2 weeks and individual volumes were measured over time. Daily TAK-242 treatment by oral gavage over 18 weeks resulted in a dose-dependent delay in the growth of these small lesions. Progression of the small lesions to tumors >7.5 mm^3 were first detected after 2 weeks in 3 of the 10 mice from the placebo and 3 mg/kg TAK-242 treatment groups as well as in 1 of the 10 mice treated with 10 mg/kg TAK-242. Among the 10 mice treated with 30 mg/kg TAK-242, progression of the small lesions to tumors >7.5 mm^3 was first detected after 4 weeks in only 1 mouse. At end of treatment, 90%, 80%, 67% and 40% of the small lesions progressed to tumors >7.5 mm^3 in the placebo, 3, 10 and 30 mg/kg TAK-242 treatment groups, respectively (p=0.02) (Fig. 3B). The significant delay in small lesions progression to tumors in mice treated with 30 mg/kg TAK-242 was further demonstrated using tumor-free survival curves, where mice with lesions <7.5 mm^3 were considered “tumor-free”. Mice treated with 30 mg/kg TAK-242 had a median tumor-free survival time of 126 days compared to 63 for mice in the placebo group (p=0.010) (Fig. 3C). Tumor volumes and tumor burden in each treatment group at necropsy, together with average curves of growth over the course of the treatment, are shown in Fig. 3D–E. At end of treatment, average tumor volume was strongly reduced in all TAK-242 treatment groups compared to placebo. The strongest reductions were observed for mice in the 10 (21.3-fold) and 30 (9.7-fold) mg/kg TAK-252 treatment groups. Average tumor volume at end of treatment was 581.0, 159.2, 27.2 and 59.8 mm^3 for placebo, 3, 10 and 30 mg/kg TAK-242 treatment groups, respectively (p=0.035). Tumor histology was also assessed for pre-existing lesions collected at time of necropsy after 18 weeks of treatment. There were no significant differences in the proportion of lesions classified as carcinomas between each treatment group versus placebo (Supplementary Fig. S3). These data indicated that 18-week treatment of Hep*Pten*$^{-}$ mice with TAK-242 resulted in reduced progression of small pre-HCC lesions.

Liver Histology and Liver Injury Markers in Hep*Pten*$^{-}$ Mice Treated with TAK-242

Histology of all livers collected at time of necropsy was blindly evaluated for parameters of NASH and liver fibrosis (Fig. 4A). Macrovesicular steatosis was significantly reduced in livers of mice treated with 30 mg/kg TAK-242 compared to placebo (scores=1.16 vs 1.65; 32% vs 65% of scores ≥2, p=0.05). An improvement in microvesicular steatosis was also observed following 30 mg/kg TAK-242 treatment but did not reach significance. In addition, treatment with 30 mg/kg TAK-242 resulted in reduced lobular inflammation (scores=1.42 vs 1.75; 37% vs 65% of scores ≥2) and reduced hepatocellular ballooning (scores=1.31 vs 1.7; 53% vs 75% of score 2). As a result, NASH severity, estimated by modified NAS, was reduced following treatment with 30 mg/kg TAK-242 (scores=6.1 vs 7.6; 32% vs 60% of scores ≥ 8). No effect of TAK-242 treatment on bile ductular reaction or liver fibrosis was observed.

Serum liver injury markers AST and ALT were also measured. While no significant changes in AST were observed in TAK-242 treatment groups compared to placebo, lower levels of ALT were observed in all TAK-242 treatment groups, reaching significance in the 30 mg/kg TAK-242 treatment group. The median concentration of ALT in the placebo group was 462 U/L versus 339 U/L, 312 U/L and 327 U/L in the 3, 10 and 30 mg/kg TAK-242 treatment groups, respectively (p=0.032) (Fig. 4B). Overall, 18-week treatment of Hep*Pten*$^{-}$ mice with 30 mg/kg TAK-242 led to reduced macrovesicular steatosis and serum levels of ALT.

TAK-242-Induced Hepatic Gene Expression Changes that Correlate with HCC Prevention Efficacy

To determine gene expression changes that may mediate TAK-242-induced HCC prevention, RNA sequencing was performed on liver tissue from mice treated with placebo or 30 mg/kg TAK-242 for 18 weeks. 220 TAK-242-induced DEGs that also had a significant correlation with tumor burden by Spearman correlation analysis were identified (Fig. 5, Supplementary Table S2). Among them, 42 were upregulated upon TAK-242 treatment and negatively correlated with tumor burden, while 178 were downregulated upon TAK-242 treatment and positively correlated with tumor burden. Hierarchical clustering based on these 220 genes successfully distinguished placebo-treated livers from TAK-242-treated livers (Fig. 5A). Genes strongly upregulated or with strong negative correlation with tumor burden included: cytochrome P450 genes (*CYP2B13; CYP2B9; CYP2C55*) [FC=3.5 (p=0.007), r_s=−0.57 (p=0.023); FC=2.7 (p=0.002), r_s=−0.57 (p=0.024); FC=1.5 (p=0.050), r_s=−0.87 (p<0.001)], metabotropic glutamate receptor 8 (*GRM8*) [FC=3.2 (p=0.015), r_s=−0.61 (p=0.014)], long non-coding RNA predicted gene 12718 (*GM12718*) [FC=2.5 (p=0.028), r_s=−0.74 (p=0.002)], S100 calcium binding protein G (*S100G*) [FC=2.5 (p=0.015), r_s=−0.57 (p=0.023)] and carboxylesterase 1G (*CES1G*) [FC=2.3 (p=0.021), r_s=−0.62 (p=0.013)], kielin/chordin-like protein (*KCP*) [FC=1.6 (p=0.005), r_s=−0.78 (p=0.001)], ankyrin repeat and SOCS box-containing 16 (*ASB16*) [FC=1.6 (p=0.038), r_s=−0.77 (p=0.001)], and cytoskeleton associated protein 2 (*CKAP2*) [FC=1.6 (p=0.028), r_s=−0.75 (p=0.001)]. Genes strongly downregulated or with strong positive correlation with tumor burden included: RNA binding motif protein 24 (*RBM24*) [FC=−8.2 (p=0.001), r_s=0.67 (p=0.006)], immunoglobulin heavy variable V1–42 (*IGHV1–42*) [FC=−7.9 (p=0.010), r_s=0.58 (p=0.022)], methyltransferase-like 7A2 (*METTL7A2*) [FC=−4.5 (p<0.001), r_s=0.62 (p=0.013)], peptidoglycan recognition protein 4 (*PGLYRP4*) [FC=−4.4 (p=0.050), r_s=0.62 (p=0.012)] and POU Class 3 Homeobox 1 *(POU3F1)* [FC=−4.0 (p=0.007), r_s=0.53 (p=0.037)], ATPase genes (*ATP6V1B1; ATP10B*) [FC=−3.9 (p=0.007), r_s=0.59 (p=0.019); FC=−2.3 (p=0.010), r_s=0.81 (p<0.001)], the long non-coding RNA *H19* [FC=−2.6 (p=0.021), r_s=0.51 (p=0.045)], keratin 19 (*KRT19*) [FC=−1.5 (p=0.003), r_s=0.65 (p=0.008)], paired-Ig-like receptor A2 (*PIRA2*) [FC=−1.5 (p=0.021), r_s=0.84 (p<0.001)], glutamate-rich protein 5 (*ERICH5*) [FC=−2.0 (p=0.007), r_s=0.82 (p<0.001)], surfactant associated protein D (*SFTPD*) [FC=−2.4 (p=0.001), r_s=0.81 (p<0.001)], and Rho GTPase activating protein 8 (*ARHGAP8*) [FC=−2.1 (p=0.010), r_s=0.80 (p<0.001)].

For each liver sample, the relative proportions of different cell types were inferred based on RNA sequencing profiles (Fig. 6A). Mice treated with 30 mg/kg TAK-242 had significantly decreased relative proportions of endothelial cells (5.4% vs 7.2%, p=0.012), Kupffer cells

(3.0% vs 3.5%, p=0.049), Siglec-H high dendritic cells (DCs) (1.7% vs 2.2%, p=0.049) and neutrophilic granule protein (*NGP*) high neutrophils (0.13% vs 0.26%, p=0.036). Conversely, there was an increase in the proportion of the minor subset of hepatocytes with high expression of mitochondrial NADH dehydrogenase 4 (*MT-ND4*) (1.7% vs 0.9%, p=0.010) (Fig. 6B). Importantly, the relative proportions of *NGP* high neutrophils and endothelial cells positively correlated with tumor burden [r_s=0.70 (p=0.003) and r_s=0.62 (p=0.011), respectively], while the proportion of *MT-ND4* high hepatocytes negatively correlated with tumor burden at necropsy [r_s=−0.53 (p=0.037)] (Fig. 6C). Overall, 18-week treatment of Hep*Pten*$^{-}$ mice with 30 mg/kg TAK-242-induced hepatic gene expression changes that significantly correlated with tumor burden, as well as changes in the proportion of various cell populations in the mouse liver.

DISCUSSION

In this study, we aimed to determine the optimal oral delivery of TAK-242 and its tolerability and efficacy in preventing NASH-associated HCC in the Hep*Pten*$^{-}$ mouse model. The optimal dose of TAK-242 was determined to be 30 mg/kg in an oral formulation of 5% DMSO in 30% 2-HPβCD. The 30 mg/kg dosage had the largest detection range compared to 3 and 10 mg/kg, and was well-tolerated over a long duration of 18 weeks. Efficacy studies demonstrated a significant delay in tumor development in Hep*Pten*$^{-}$ mice treated with 30 mg/kg TAK-242. Individual tumor volumes and total tumor burdens were strongly reduced at end of treatment, confirmed by both MRI and necropsy measurements. Furthermore, in Hep*Pten*$^{-}$ mice with small pre-existing adenomas at start of treatment, a dose-dependent effect of TAK-242 on progression to HCC was observed. Individual volumes of pre-existing lesions were significantly lower at 4 out of 10 MRI timepoints for 10 mg/kg TAK-242-treated mice and 8 out of 10 MRI timepoints for 30 mg/kg TAK-242-treated mice. Mice treated with 30 mg/kg TAK-242 also displayed significantly lower tumor volumes of pre-existing lesions at necropsy. Overall, these results indicate a dose-dependent relationship between TAK-242 and suppression of tumor development, even from pre-existing adenomas. These findings were accompanied by reduced steatosis and serum levels of ALT, indicative of an improvement in underlying liver pathology.

To elucidate the mechanisms of TAK-242-mediated HCC prevention, we determined the changes in hepatic expression profiles upon treatment that also correlated with tumor burden. Several cytochrome P450 genes and *CES1G* were upregulated, indicating xenobiotic metabolism in response to TAK-242 administration. *CES1G* also possesses triglyceride hydrolase activity and has been shown to improve liver steatosis, lipid homeostasis, insulin signaling and liver inflammation (31). Another upregulated gene of interest with negative correlation with tumor burden was *S100G*, a vitamin D-dependent calcium-binding protein. High expression of *S100G* in HCC has been associated with improved overall survival (32). The greatest decrease in expression was observed for *RBM24*, an RNA-binding protein involved in post-transcriptional regulation of gene expression. Both tumor suppressive and tumor promoting functions for *RBM24* in HCC have been reported (33). Significant downregulation of *IGHV1-45* and other genes from the immunoglobulin heavy and kappa locus was observed, suggesting reduced immunoglobulin production by B cells. Of interest, the B cell population size in the liver was unchanged upon TAK-242 treatment. TLR4

signaling has been shown to augment activation of B cells and regulate immunoglobulin production (34). Elevated level of circulating immunoglobulins was observed in NASH patients and positively associated with fibrosis severity and mortality (35, 36). TAK-242 treatment also led to downregulation of several other genes previously associated with HCC, namely *ATP6V1B1*, *H19*, and *KRT19*. *ATP6V1B1*, a component of vacuolar ATPase, is upregulated in HCC and may promote cancer cells survival by regulating acidity in the tumor microenvironment (37). *H19* is a long non-coding RNA with a well-established role in promoting NAFLD (38). Its role in HCC remains however controversial, with potential tumor suppressive or promoting effects (39). *KRT19*, a marker of biliary epithelial cells, reflects this cell of origin in a subset of HCC with poor prognosis. High *KRT19* expression has been associated with HCC tumor size, cell de-differentiation, metastasis and poor prognosis (40).

Based on inferred cell populations from bulk liver RNA sequencing data, TAK-242 treatment was accompanied by decreased populations of endothelial cells and several myeloid-derived immune cell types (Kupffer cells, Siglec-H high DCs and *NGP* high neutrophils). Furthermore, the proportion of *NGP* high neutrophils and endothelial cells positively correlated with tumor burden. Kupffer cells, the resident macrophages and largest population of immune cells in the liver, are potential drivers of fibrogenesis. Enrichment of Kupffer cells in the liver has been observed with increasing NASH and fibrosis severity in NAFLD patients (41, 42). Hepatic DCs are divided into two main classes in both mice and humans: classical and plasmacytoid. Plasmacytoid DCs, characterized by expression of Siglec-H, are the most abundant subset in the mouse liver and function as a major source of type I interferons (43). Kupffer cells and plasmacytoid DCs express TLR4 and produce proinflammatory TNF-α and IL-6 upon TLR4 signaling (44). Neutrophils are recruited to the liver in chronic liver disease, driving hepatocyte damage and promoting inflammation (45). Collectively, a reduction in these cell populations could mediate the attenuated hepatic inflammatory environment induced by TLR4 inhibition. Conversely, we observed a significantly increased proportion of *MT-ND4* high hepatocytes in mice treated with TAK-242, which also negatively correlated with tumor burden. This recently identified minor subset of hepatocytes is characterized by high expression mitochondrial genes (46). *MT-ND4* is part of the mitochondrial respiratory chain complex I required for oxidative phosphorylation. Changes in this cell population suggest that TLR4 inhibition induces alterations in mitochondrial function, oxidative phosphorylation and reactive oxygen species production, key processes that contribute to the development of NASH (47–49).

In conclusion, inhibition of TLR4 by the small molecular inhibitor TAK-242 was well-tolerated and reduced the development of HCC and progression of small pre-existing adenomas in the Hep*Pten*$^{-}$ mouse model of NASH-associated HCC. TLR4 inhibition was accompanied by changes in hepatic expression of 220 genes that correlated with tumor burden. It also resulted in depletion of neutrophils and endothelial cells and enrichment of MT-ND4 high hepatocytes, indicative of alleviation of hepatic inflammation and increased mitochondrial function and oxidative phosphorylation. These studies support further development of TAK-424 for the prevention of HCC in individuals with NASH. Additional early studies in humans will be needed to determine the toxicity and tolerability of TLR4 inhibitors in this population. These studies also provide novel insights into

molecular and cellular events associated with HCC development in NASH that merit further investigations. Future studies should also focus on developing a pharmacodynamic signature of TLR4 inhibition as well as on demonstrating that HCC prevention by TAK-242 is solely mediated by TLR4 inhibition.

Supplementary Material

Refer to Web version on PubMed Central for supplementary material.

ACKNOWLEDGMENTS

This research was supported by the National Cancer Institute PREVENT Cancer Program contract HHSN261201500018I to L. Beretta, and by the MD Anderson Cancer Center SPORE in Hepatocellular Carcinoma Grant P50 CA217674 to L. Beretta. The MD Anderson Advanced Technology Genomics Core is supported by the MD Anderson Cancer Center Support Grant CA016672 from the National Cancer Institute and the National Institutes of Health grant 1S10OD024977-01. The Gulf Coast Consortia Center for Comprehensive PK/PD & Formulation Core is funded by CPRIT grant RP180748 to D. Liang.

List of Abbreviations

2-HPβCD	2-hydroxypropyl-β-cyclodextrin
ALT	Alanine aminotransferase
AST	Aspartate aminotransferase
CBC	Complete blood count
CMC	Carboxymethyl cellulose
CPM	Counts per million
DEG	Differentially-expressed gene
DMSO	Dimethyl sulfoxide
GADPH	Glyceraldehyde-3-phosphate dehydrogenase
HCC	Hepatocellular carcinoma
HPLC	High-performance liquid chromatography
HPMC	Hydroxypropylmethylcellulose
IL-10	Interleukin 10
IL-6	Interleukin 6
IP	Intraperitonea
LC-MS/MS	Liquid chromatography with tandem mass spectrometry
K2 EDTA	dipotassium ethylenediaminetetraacetic acid
MRI	Magnetic resonance imaging

NAFLD	Non-alcoholic fatty liver disease
NAS	NAFLD activity score
NASH	Non-alcoholic steatohepatitis
PCR	Polymerase chain reaction
PD	Pharmacodynamic
PK	Pharmacokinetic
PTEN	Phosphatase and tensin homolog
TLR4	Toll-like receptor 4
TNF-α	Tumor necrosis factor alpha

REFERENCES

1. Ferlay J, Soerjomataram I, Dikshit R, Eser S, Mathers C, Rebelo M, et al. Cancer incidence and mortality worldwide: sources, methods and major patterns in GLOBOCAN 2012. Int J Cancer. 2015;136(5):E359–86. [PubMed: 25220842]
2. Wallace MC, Preen D, Jeffrey GP, Adams LA. The evolving epidemiology of hepatocellular carcinoma: a global perspective. Expert review of gastroenterology & hepatology. 2015;9(6):765–79. [PubMed: 25827821]
3. Ryerson AB, Eheman CR, Altekruse SF, Ward JW, Jemal A, Sherman RL, et al. Annual Report to the Nation on the Status of Cancer, 1975–2012, featuring the increasing incidence of liver cancer. Cancer. 2016;122(9):1312–37. [PubMed: 26959385]
4. Younossi ZM, Stepanova M, Younossi Y, Golabi P, Mishra A, Rafiq N, et al. Epidemiology of chronic liver diseases in the USA in the past three decades. Gut. 2020;69(3):564–8. [PubMed: 31366455]
5. Estes C, Anstee QM, Arias-Loste MT, Bantel H, Bellentani S, Caballeria J, et al. Modeling NAFLD disease burden in China, France, Germany, Italy, Japan, Spain, United Kingdom, and United States for the period 2016–2030. Journal of hepatology. 2018;69(4):896–904. [PubMed: 29886156]
6. Siegel RL, Miller KD, Fuchs HE, Jemal A. Cancer statistics, 2022. CA: a cancer journal for clinicians. 2022;72(1):7–33. [PubMed: 35020204]
7. Huang DQ, El-Serag HB, Loomba R. Global epidemiology of NAFLD-related HCC: trends, predictions, risk factors and prevention. Nature reviews Gastroenterology & hepatology. 2021;18(4):223–38. [PubMed: 33349658]
8. Lange NF, Radu P, Dufour JF. Prevention of NAFLD-associated HCC: Role of lifestyle and chemoprevention. Journal of hepatology. 2021;75(5):1217–27. [PubMed: 34339764]
9. Horie Y, Suzuki A, Kataoka E, Sasaki T, Hamada K, Sasaki J, et al. Hepatocyte-specific Pten deficiency results in steatohepatitis and hepatocellular carcinomas. J Clin Invest. 2004;113(12):1774–83. [PubMed: 15199412]
10. Stiles B, Wang Y, Stahl A, Bassilian S, Lee WP, Kim YJ, et al. Liver-specific deletion of negative regulator Pten results in fatty liver and insulin hypersensitivity [corrected]. Proc Natl Acad Sci U S A. 2004;101(7):2082–7. [PubMed: 14769918]
11. Nguyen J, Jiao J, Smoot K, Watt GP, Zhao C, Song X, et al. Toll-like receptor 4: a target for chemoprevention of hepatocellular carcinoma in obesity and steatohepatitis. Oncotarget. 2018;9(50):29495–507. [PubMed: 30034633]
12. Carpino G, Del Ben M, Pastori D, Carnevale R, Baratta F, Overi D, et al. Increased Liver Localization of Lipopolysaccharides in Human and Experimental NAFLD. Hepatology. 2020;72(2):470–85. [PubMed: 31808577]

13. Zhu Q, Zou L, Jagavelu K, Simonetto DA, Huebert RC, Jiang ZD, et al. Intestinal decontamination inhibits TLR4 dependent fibronectin-mediated cross-talk between stellate cells and endothelial cells in liver fibrosis in mice. Journal of hepatology. 2012;56(4):893–9. [PubMed: 22173161]
14. Liu WT, Jing YY, Gao L, Li R, Yang X, Pan XR, et al. Lipopolysaccharide induces the differentiation of hepatic progenitor cells into myofibroblasts constitutes the hepatocarcinogenesis-associated microenvironment. Cell Death Differ. 2020;27(1):85–101. [PubMed: 31065105]
15. Yu J, Zhu C, Wang X, Kim K, Bartolome A, Dongiovanni P, et al. Hepatocyte TLR4 triggers inter-hepatocyte Jagged1/Notch signaling to determine NASH-induced fibrosis. Science translational medicine. 2021;13(599).
16. Liu B, Xiang L, Ji J, Liu W, Chen Y, Xia M, et al. Sparcl1 promotes nonalcoholic steatohepatitis progression in mice through upregulation of CCL2. The Journal of clinical investigation. 2021;131(20).
17. Ye D, Li FY, Lam KS, Li H, Jia W, Wang Y, et al. Toll-like receptor-4 mediates obesity-induced non-alcoholic steatohepatitis through activation of X-box binding protein-1 in mice. Gut. 2012;61(7):1058–67. [PubMed: 22253482]
18. Dapito DH, Mencin A, Gwak GY, Pradere JP, Jang MK, Mederacke I, et al. Promotion of hepatocellular carcinoma by the intestinal microbiota and TLR4. Cancer Cell. 2012;21(4):504–16. [PubMed: 22516259]
19. Loh JJ, Li TW, Zhou L, Wong TL, Liu X, Ma VWS, et al. FSTL1 Secreted by Activated Fibroblasts Promotes Hepatocellular Carcinoma Metastasis and Stemness. Cancer research. 2021;81(22):5692–705. [PubMed: 34551961]
20. Chen CL, Tsukamoto H, Liu JC, Kashiwabara C, Feldman D, Sher L, et al. Reciprocal regulation by TLR4 and TGF-beta in tumor-initiating stem-like cells. The Journal of clinical investigation. 2013;123(7):2832–49. [PubMed: 23921128]
21. Takashima K, Matsunaga N, Yoshimatsu M, Hazeki K, Kaisho T, Uekata M, et al. Analysis of binding site for the novel small-molecule TLR4 signal transduction inhibitor TAK-242 and its therapeutic effect on mouse sepsis model. British journal of pharmacology. 2009;157(7):1250–62. [PubMed: 19563534]
22. Qian Y, Han J, Zhou L, Yu Q, Xu J, Jin Z, et al. Inhibition of Epidermal Growth Factor Receptor (EGFR) Reduces Lipopolysaccharide (LPS)-Induced Activation and Inflammatory Cytokines in Hepatic Stellate Cells In Vitro. Medical science monitor : international medical journal of experimental and clinical research. 2018;24:5533–41. [PubMed: 30091424]
23. Engelmann C, Sheikh M, Sharma S, Kondo T, Loeffler-Wirth H, Zheng YB, et al. Toll-like receptor 4 is a therapeutic target for prevention and treatment of liver failure. Journal of hepatology. 2020;73(1):102–12. [PubMed: 31987990]
24. Kramer B, Franca LM, Zhang Y, Paes AMA, Gerdes AM, Carrillo-Sepulveda MA. Western diet triggers Toll-like receptor 4 signaling-induced endothelial dysfunction in female Wistar rats. Am J Physiol Heart Circ Physiol. 2018;315(6):H1735–H47. [PubMed: 30265151]
25. Wang H, Li X, Dong G, Yan F, Zhang J, Shi H, et al. Toll-like Receptor 4 Inhibitor TAK-242 Improves Fulminant Hepatitis by Regulating Accumulation of Myeloid-Derived Suppressor Cell. Inflammation. 2021;44(2):671–81. [PubMed: 33083887]
26. Yu P, Cheng X, Du Y, Huang L, Dong R. TAK-242 can be the potential agents for preventing invasion and metastasis of hepatocellular carcinoma. Med Hypotheses. 2013;81(4):653–5. [PubMed: 23910073]
27. Zhang X, Li S, Li M, Huang H, Li J, Zhou C. Hypoxia-inducible factor-1alpha mediates the toll-like receptor 4 signaling pathway leading to anti-tumor effects in human hepatocellular carcinoma cells under hypoxic conditions. Oncol Lett. 2016;12(2):1034–40. [PubMed: 27446390]
28. Kleiner DE, Brunt EM, Van Natta M, Behling C, Contos MJ, Cummings OW, et al. Design and validation of a histological scoring system for nonalcoholic fatty liver disease. Hepatology. 2005;41(6):1313–21. [PubMed: 15915461]
29. Newman AM, Steen CB, Liu CL, Gentles AJ, Chaudhuri AA, Scherer F, et al. Determining cell type abundance and expression from bulk tissues with digital cytometry. Nat Biotechnol. 2019;37(7):773–82. [PubMed: 31061481]

30. Danaher P, Kim Y, Nelson B, Griswold M, Yang Z, Piazza E, et al. Advances in mixed cell deconvolution enable quantification of cell types in spatial transcriptomic data. Nature communications. 2022;13(1):385.
31. Xu Y, Zhu Y, Bawa FC, Hu S, Pan X, Yin L, et al. Hepatocyte-Specific Expression of Human Carboxylesterase 1 Attenuates Diet-Induced Steatohepatitis and Hyperlipidemia in Mice. Hepatol Commun. 2020;4(4):527–39. [PubMed: 32258948]
32. Zhang C, Yao R, Chen J, Zou Q, Zeng L. S100 family members: potential therapeutic target in patients with hepatocellular carcinoma: A STROBE study. Medicine (Baltimore). 2021;100(3):e24135. [PubMed: 33546025]
33. Shi DL. RBM24 in the Post-Transcriptional Regulation of Cancer Progression: Anti-Tumor or Pro-Tumor Activity? Cancers. 2022;14(7).
34. Buchta CM, Bishop GA. Toll-like receptors and B cells: functions and mechanisms. Immunol Res. 2014;59(1–3):12–22. [PubMed: 24847763]
35. McPherson S, Henderson E, Burt AD, Day CP, Anstee QM. Serum immunoglobulin levels predict fibrosis in patients with non-alcoholic fatty liver disease. Journal of hepatology. 2014;60(5):1055–62. [PubMed: 24445215]
36. De Roza MA, Lamba M, Goh GB, Lum JH, Cheah MC, Ngu JHJ. Immunoglobulin G in non-alcoholic steatohepatitis predicts clinical outcome: A prospective multi-centre cohort study. World journal of gastroenterology : WJG. 2021;27(43):7563–71. [PubMed: 34887649]
37. Xu J, Xie R, Liu X, Wen G, Jin H, Yu Z, et al. Expression and functional role of vacuolar H(+)-ATPase in human hepatocellular carcinoma. Carcinogenesis. 2012;33(12):2432–40. [PubMed: 22962303]
38. Wang Y, Hylemon PB, Zhou H. Long Noncoding RNA H19: A Key Player in Liver Diseases. Hepatology. 2021;74(3):1652–9. [PubMed: 33630308]
39. Tietze L, Kessler SM. The Good, the Bad, the Question-H19 in Hepatocellular Carcinoma. Cancers. 2020;12(5).
40. Govaere O, Komuta M, Berkers J, Spee B, Janssen C, de Luca F, et al. Keratin 19: a key role player in the invasion of human hepatocellular carcinomas. Gut. 2014;63(4):674–85. [PubMed: 23958557]
41. Pantano L, Agyapong G, Shen Y, Zhuo Z, Fernandez-Albert F, Rust W, et al. Molecular characterization and cell type composition deconvolution of fibrosis in NAFLD. Scientific reports. 2021;11(1):18045. [PubMed: 34508113]
42. Park JW, Jeong G, Kim SJ, Kim MK, Park SM. Predictors reflecting the pathological severity of non-alcoholic fatty liver disease: comprehensive study of clinical and immunohistochemical findings in younger Asian patients. J Gastroenterol Hepatol. 2007;22(4):491–7. [PubMed: 17376039]
43. Rahman AH, Aloman C. Dendritic cells and liver fibrosis. Biochim Biophys Acta. 2013;1832(7):998–1004. [PubMed: 23313573]
44. Nakamoto N, Kanai T. Role of toll-like receptors in immune activation and tolerance in the liver. Frontiers in immunology. 2014;5:221. [PubMed: 24904576]
45. Weston CJ, Zimmermann HW, Adams DH. The Role of Myeloid-Derived Cells in the Progression of Liver Disease. Frontiers in immunology. 2019;10:893. [PubMed: 31068952]
46. Han X, Wang R, Zhou Y, Fei L, Sun H, Lai S, et al. Mapping the Mouse Cell Atlas by Microwell-Seq. Cell. 2018;172(5):1091–107 e17. [PubMed: 29474909]
47. Dornas W, Schuppan D. Mitochondrial oxidative injury: a key player in nonalcoholic fatty liver disease. Am J Physiol Gastrointest Liver Physiol. 2020;319(3):G400–G11. [PubMed: 32597705]
48. Mansouri A, Gattolliat CH, Asselah T. Mitochondrial Dysfunction and Signaling in Chronic Liver Diseases. Gastroenterology. 2018;155(3):629–47. [PubMed: 30012333]
49. Zhong X, Xiao Q, Liu Z, Wang W, Lai CH, Yang W, et al. TAK242 suppresses the TLR4 signaling pathway and ameliorates DCD liver IRI in rats. Mol Med Rep. 2019;20(3):2101–10. [PubMed: 31257518]

PREVENTION RELEVANCE

Means to prevent development of HCC or progression of small adenomas to HCC in patients with NASH are urgently needed to reduce the growing mortality due to HCC. We characterized the chemopreventive effect of oral administration of the TLR4 inhibitor TAK-242 in a model of NASH-associated HCC.

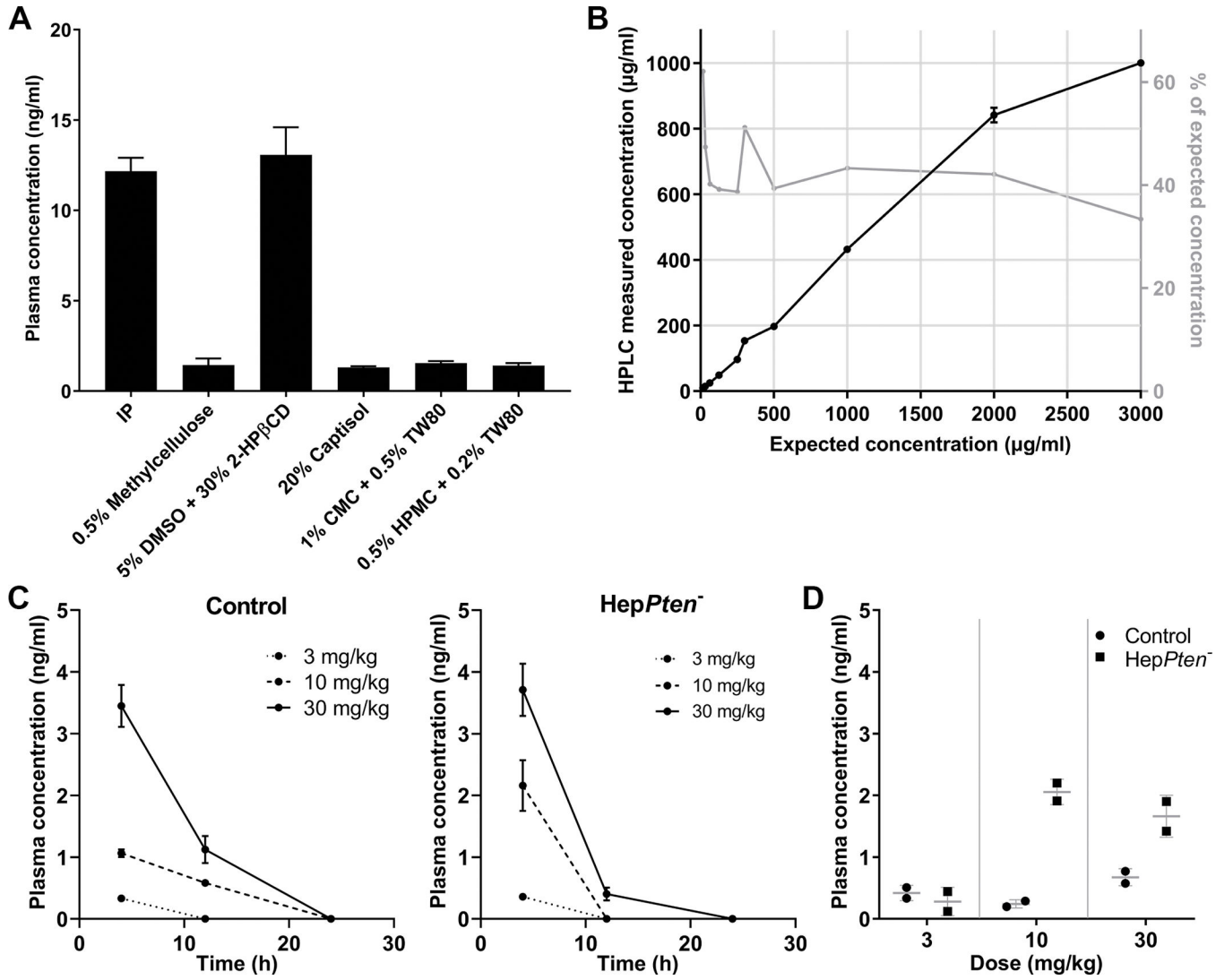

Figure 1. TAK-242 oral gavage formulations and PK studies.

(A) Plasma concentrations of TAK-242 in mice 2 hrs after administration by IP or oral gavage of TAK-242 at a dose of 15 mg/kg. The oral formulations tested were: 0.5% methylcellulose, 5% dimethyl sulfoxide in 30% 2-hydroxypropyl-β-cyclodextrin (5% DMSO + 30% 2-HPβCD), 20% captisol. 1% carboxymethyl cellulose and 0.5% Tween-80 (1% CMC + 0.5% TW80), and 0.5% hydroxypropylmethylcellulose and 0.2% Tween-80 (0.5% HPMC + 0.2% TW80). **(B)** Solubility of TAK-242 in 5% DMSO + 30% 2-HPβCD assessed by HPLC. The concentrations tested ranged from 15 to 3000 µg/ml (equivalent to a mouse dosage of 0.15–30 mg/kg). **(C)** TAK-242 was administered by oral gavage as a single dose of either 3, 10 or 30 mg/kg to control and Hep*Pten*⁻ mice and measured in plasma collected at 4, 12 and 24 hrs after administration. **(D)** TAK-242 was administered by oral gavage once daily for 5 days, at a dose of 3, 10 or 30 mg/kg to control and Hep*Pten*⁻ mice and measured in plasma collected 2 hrs after last dose administration.

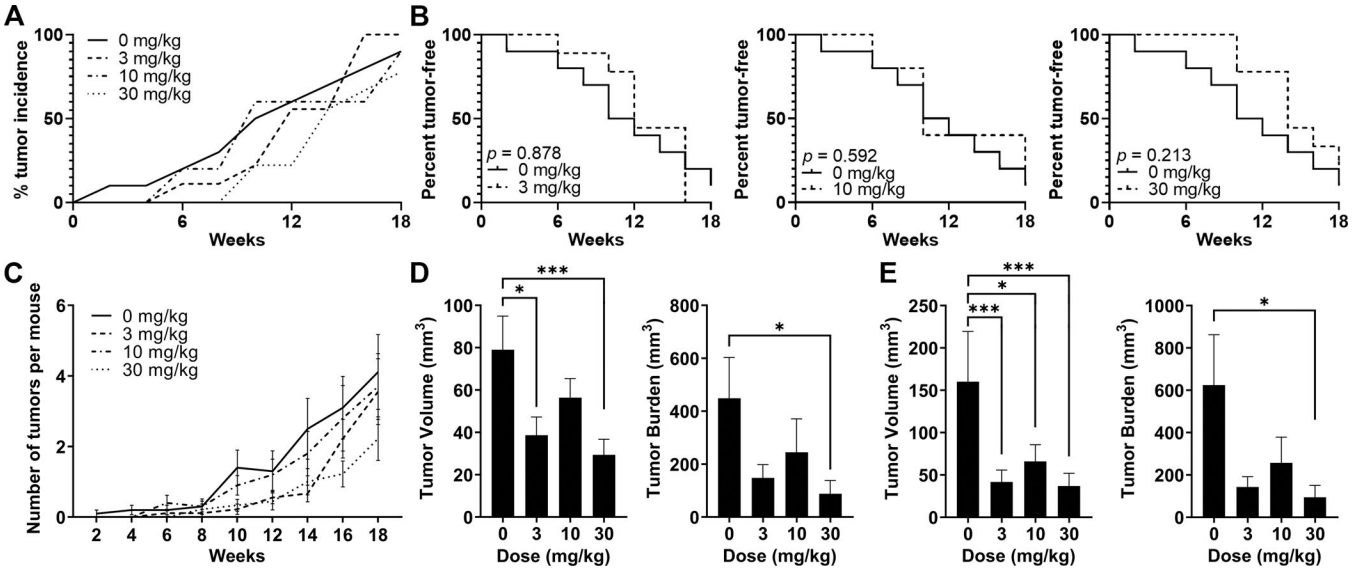

Figure 2. Prevention of liver tumor development by TAK-242 treatment in Hep*Pten*$^{-}$ mice.

Mice under treatment for 18 weeks received MRI scans every 2 weeks. Lesions >7.5 mm^3 were included in the analysis. **(A)** Tumor incidence within each treatment group at each MRI timepoint. **(B)** Tumor-free survival curves for each TAK-242 treatment group compared to placebo. Significant differences between groups were assessed by the log-rank test. **(C)** Number of tumors per mouse detected at each MRI timepoint in each treatment group. Data are shown as mean, SEM. **(D-E)** Tumor burden and individual tumor volumes at end of treatment measured **(D)** by MRI, and **(E)** at necropsy. Tumor burden was calculated as the sum of all individual tumor volumes in each mouse. Significant differences between groups were assessed by the Mann-Whitney *U* test. * p<0.05, ** p<0.01, *** p<0.001.

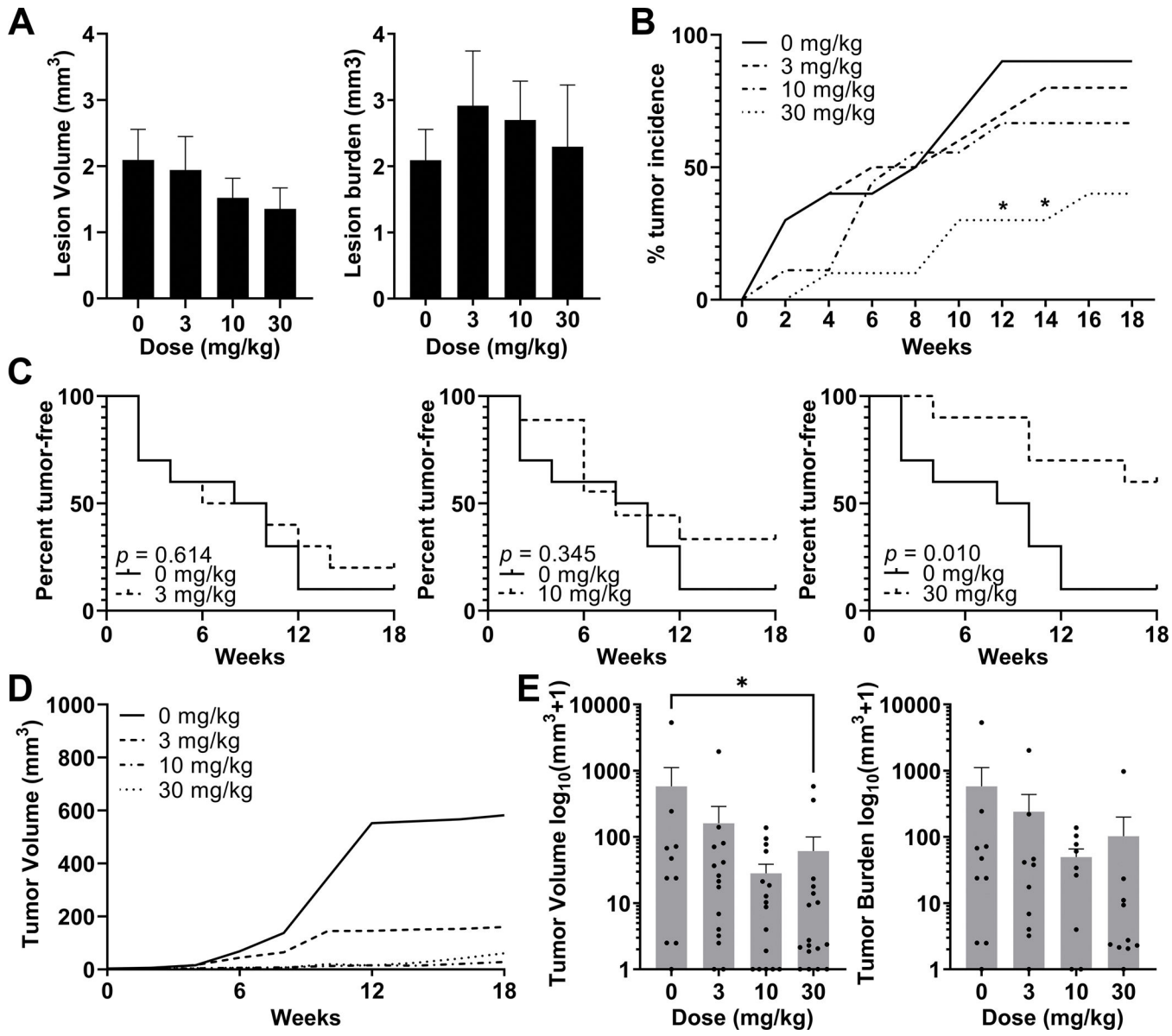

Figure 3. Prevention of progression of pre-HCC lesions by TAK-242.

Mice with lesions <7.5 mm^3 were enrolled and treated with TAK-242 at 3, 10 or 30 mg/kg for 18 weeks. All mice received MRI scans every 2 weeks. Preexisting lesions were considered tumors when they surpassed 7.5 mm^3. **(A)** Average volume of individual lesions (left) and average lesion burden, calculated as the sum of all individual lesion volumes in each mouse (right), at start of treatment in each treatment group. **(B)** Tumor incidence within each treatment group at each MRI time-point. Significant differences were assessed by Fisher's exact test. **(C)** Tumor-free survival curves for each treatment group. Significant differences between groups were assessed by log-rank test. **(D)** Tumor volume as measured by MRI over time in each treatment group. **(E)** Tumor burden and tumor volume measurements taken at time of necropsy, after 18 weeks of treatment with TAK-242. Tumor

burden was calculated as the sum of all individual tumor volumes in each mouse. Significant differences between groups were assessed by the Mann-Whitney *U* test. * $p<0.05$.

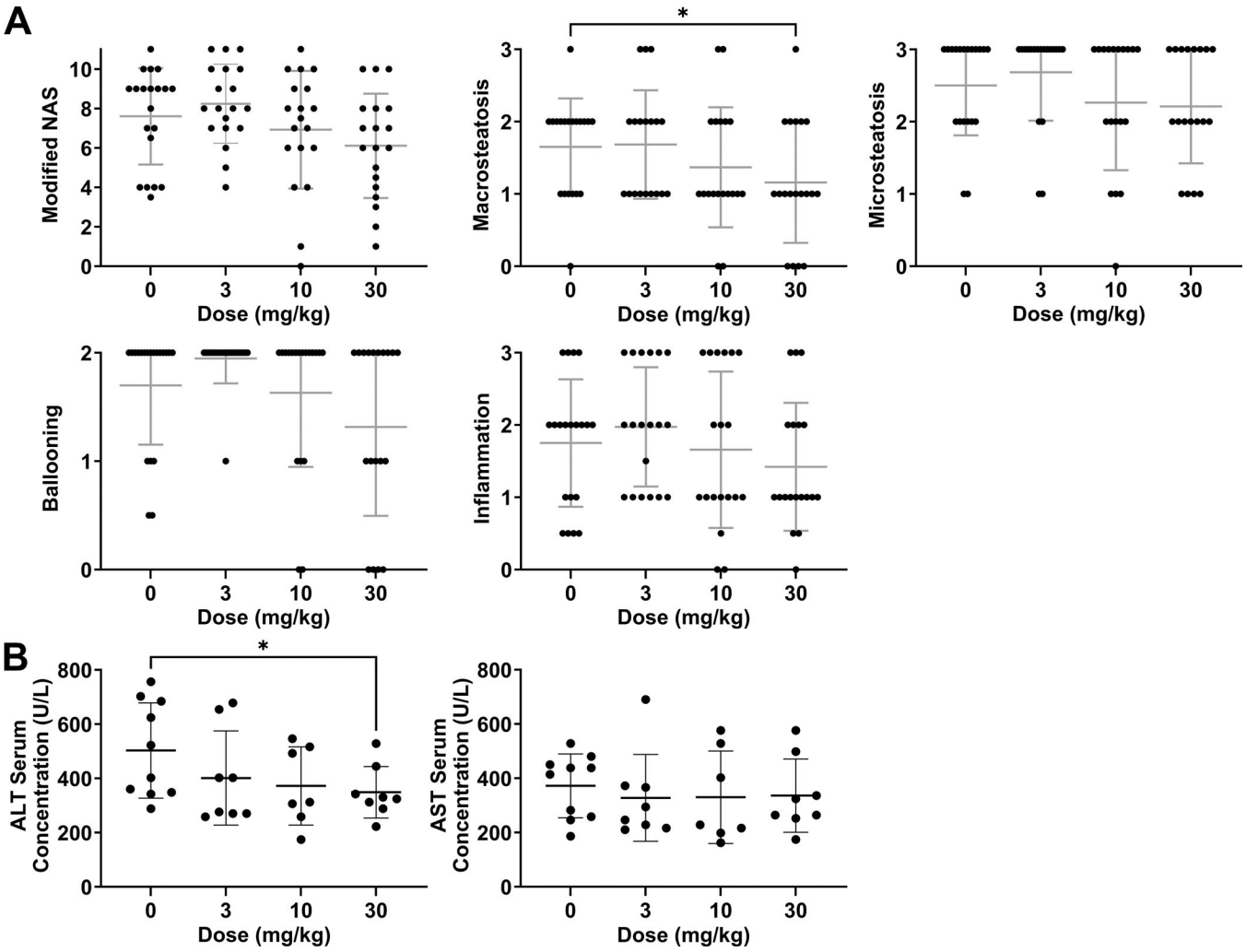

Figure 4. Liver histology and serum levels of liver injury markers in Hep*Pten*$^{-}$ mice treated with TAK-242.

(A) Livers collected at necropsy were blindly evaluated for modified NAFLD activity score (NAS; 0–11), macrovesicular steatosis (0–3), microvesicular steatosis (0–3), hepatocellular ballooning (0–2), and lobular inflammation (0–3). Significant differences between groups were assessed by unpaired *t*-test. **(B)** AST and ALT measurements in serum collected at necropsy. Significant differences between groups were assessed by the Mann-Whitney *U* test. * $p<0.05$.

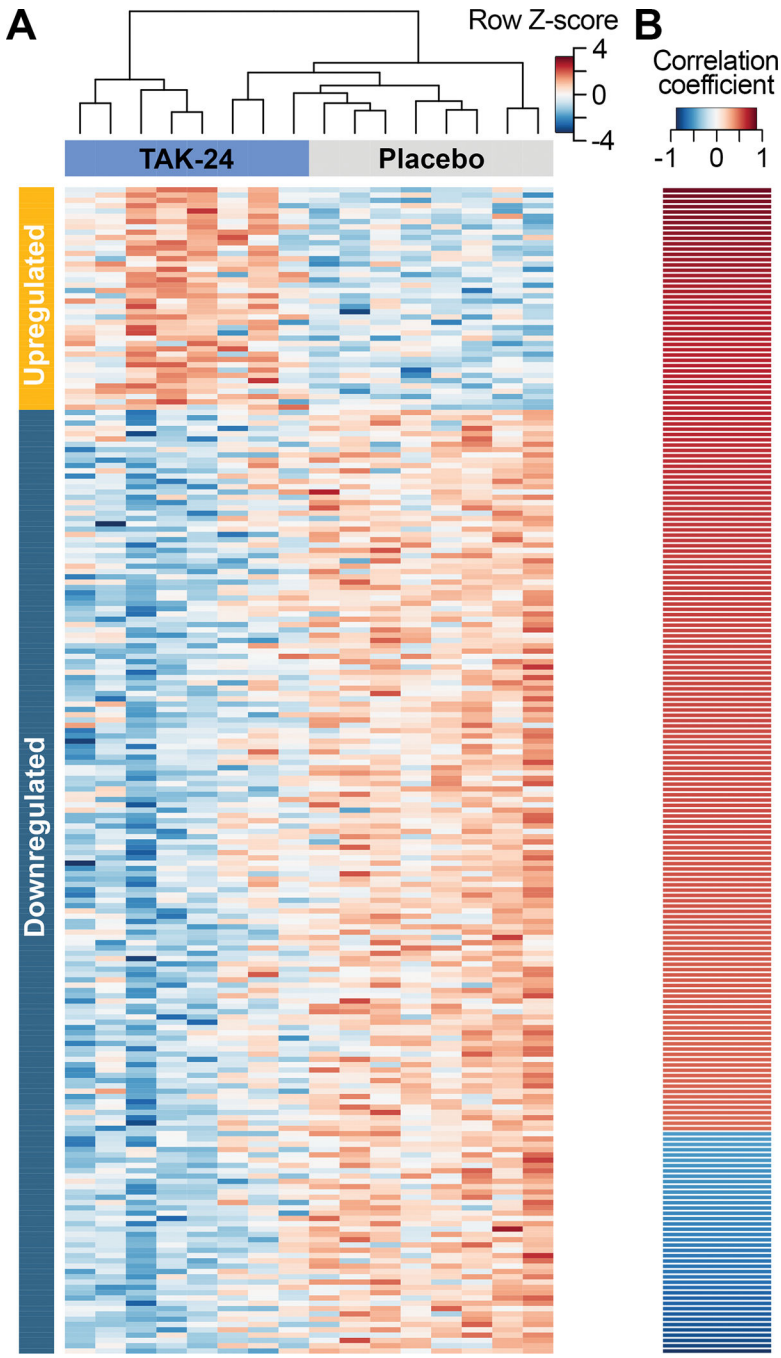

Figure 5. Differentially expressed genes with significant correlations with tumor burden at necropsy.

(A) Hierarchical clustering based on log2 counts per million of 220 DEGs in mice treated with 30 mg/kg TAK-242, and with a significant correlation with tumor burden. **(B)** Spearman's correlation of tumor burden for all 220 DEGs. Genes are sorted by correlation coefficient.

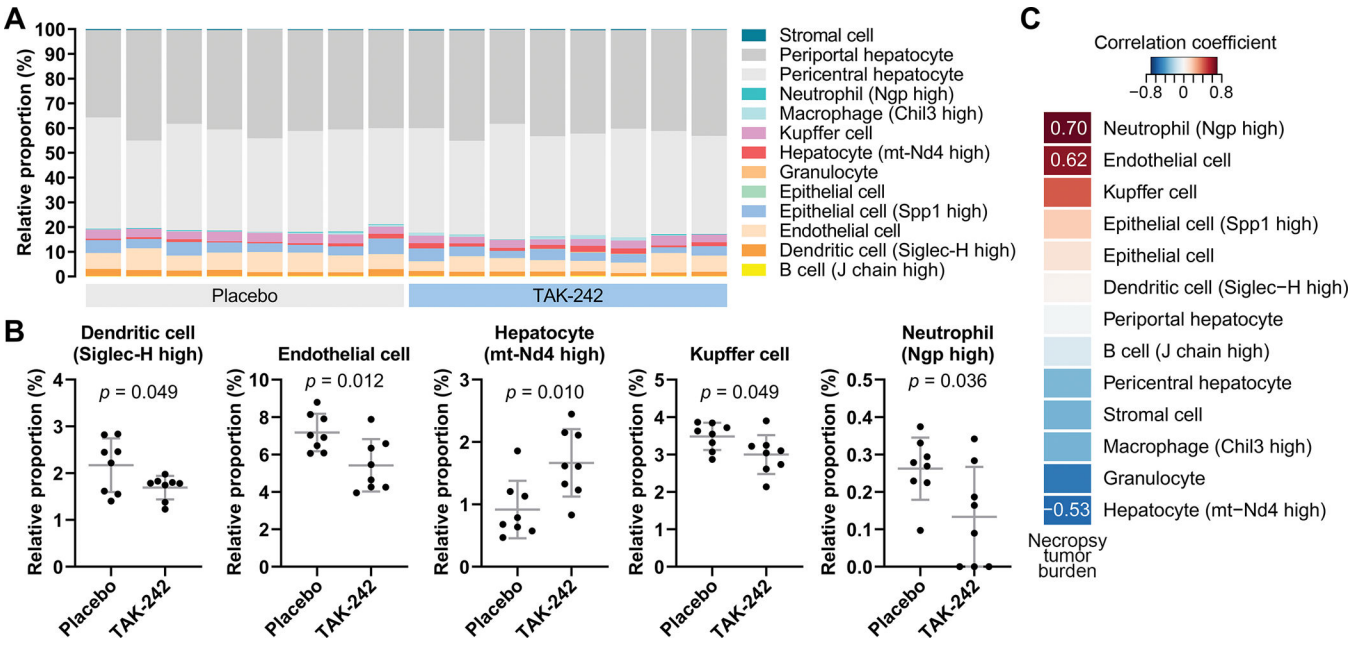

Figure 6. Changes in cell populations upon TAK-242 treatment.

(A) Cell deconvolution based on transcriptomic profiles of livers from mice treated with placebo or 30 mg/kg TAK-242. **(B)** Cell types with significantly different estimated proportions between livers of mice treated with placebo versus 30 mg/kg TAK-242. Significant differences between groups were assessed by unpaired *t*-test. **(C)** Spearman's correlation of tumor burden with all detected cell types. Cell types are sorted by correlation coefficient. Correlation coefficients are shown for correlations with Spearman's $p<0.05$.